

SURFACE TEMPERATURE AND HEAT FLUX VARIABILITY AND THEIR CHANGES WITH GLOBAL WARMING

Bin Yu and George J. Boer

Canadian Centre for Climate Modelling and Analysis, Meteorological Service of Canada
University of Victoria, PO Box 1700, Victoria, BC V8W 2Y2, Canada
Bin.Yu@ec.gc.ca; George.Boer@ec.gc.ca

1. INTRODUCTION

Sea surface temperature (SST) mediates the energy exchange at the air-sea interface and the variability of SST on different timescales reflects this coupling. This study analyzes the SST variability and its change with global warming. We directly relate the large-scale features of SST variability and heat flux (HF) variability based on both the NCEP/NCAR reanalyses and the results of the CCCma coupled atmosphere-ocean model.

2. DATA AND METHODOLOGY

The CCCma coupled model, control climate, forcing scenarios, and the simulated climate change are described in Flato et al.(2000) and Boer et al.(2000a,b). We use three 1000-yr model outputs, including the control run (CTRL) and two stabilization integrations with the forcing “stabilized” at year 2050 and 2100 values (referred to as STAB-2050 and STAB-2100, respectively). The NCEP/NCAR reanalyses monthly data, which cover the 50-yr period 1949-1998, are also employed (Kistler et al. 2001).

The energy balance of the upper layer of the ocean, after subtracting out climatological mean values of the terms, is $\frac{C\{T_d'(t + \Delta t) - T_d'(t)\}}{\Delta t} = R' + B' + A'$. Where C is the oceanic heat capacity, T the surface temperature, R and B the radiative and turbulent energy exchanges across the surface, and A the convergence of heat in the layer by transport processes (Boer, 1993). The temperatures on the *lhs* of the equation are daily values while the *rhs* terms are monthly means. When the equation is squared and averaged, the *lhs* takes the form $\frac{2C^2}{\Delta t^2} \overline{T_d'^2}_{\{1-r(\Delta t)\}}$ where r is the lagged autocorrelation. We connect the daily variability

to the variability of the monthly mean with the relationship $\overline{T^2} = \frac{\overline{T_d'^2}}{\Delta t}(1+D)$ where $D = 2 \sum_{\tau=1}^{\Delta t} \left(1 - \frac{\tau}{\Delta t}\right)r(\tau)$ involves

the lagged autocorrelations of daily values (von Storch and Zwiers, 1998). Thus the monthly mean temperature variance is related to the variance of forcing terms as

$$\overline{T^2} = G(R' + B' + A')^2 \quad \text{or} \quad \sigma_T^2 = G(\sigma_R^2 + \sigma_B^2 + \sigma_A^2)e = G\sigma_o^2e \quad (1)$$

where the transfer factor G depends on the autocorrelation structure of temperature, and σ_o^2 is the sum of the surface heat flux variances and the variance of oceanic heat flux convergence. σ_o^2 gives the contribution to the generation of temperature variance that would apply if the components were independent of one another, while e (the “efficiency” factor) measures the degree to which these physical forcing mechanisms act to counteract one another.

3. RESULTS

The surface energy budget from the control simulation is reasonably similar to observational estimates (Boer, 1993; Yu and Boer, 2002), although observation-based net HF and individual flux components still exhibit considerable differences (e.g. Trenberth et al., 2001). In some ways, the variability of HF is easier to estimate than the mean fluxes themselves. Systematic errors and biases in the means are of less importance and the main spatial scales of longer term variability tend to be large (WCRP, 2000). Figure 1 compares the results of SST variability and associated HF variability, based on (1), between CTRL and NCEP reanalyses. The qualitatively similar features are clear evident, though the modelled tropical variability is weak especially in the equatorial eastern Pacific. The configuration of σ_o^2 largely determines the SST variability. Nevertheless, it is important that the overall effect of G^*e also exhibits a spatial distribu-

tion bearing a resemblance to the spatial pattern of SST variability, indicating that they are not negligible contributors in determining the temperature variability.

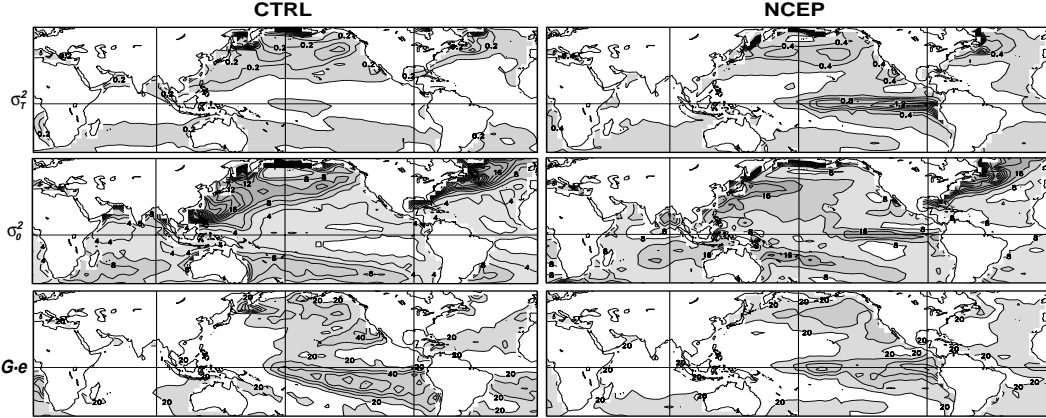


Figure 1 Geographical distributions of SST variances (σ_T^2 , $^{\circ}\text{C}^2$), the total HF variances (σ_o^2 , $10^2\text{W}^2\text{m}^{-4}$), and $G^*\text{e}$ ($10^{-50}\text{C}^2/\text{W}^2\text{m}^{-4}$) from the control simulation (CTRL) and NCEP reanalyses.

Figure 2 displays the percentage change of SST variability and variability budget terms with global

warming, $\frac{\delta\sigma_T^2}{\sigma_T^2} = \frac{\delta\sigma_0^2}{\sigma_0^2} + \frac{\delta G}{G} + \frac{\delta e}{e}$. The temperature variances are generally reduced in the tropical Pacific and enhanced in the subtropical Pacific, while enhanced variability occupies most of the Atlantic ocean. The change in HF variance σ_o^2 explains much of SST variability change, although not all. There are notable differences between the changes of SST variability and that of σ_o^2 in the tropical central Pacific, the Indian ocean and mid-latitudes of the North Atlantic. In these regions, the SST variability decreases (increases) despite an increase (decrease) in σ_o^2 and either little change or even an increase in e . The changes are associated with the transfer factor G reflecting the temperature autocorrelation structure. In the tropics, SST has a shorter memory in the warming scenarios than that in the current climate, resulting in a decreasing of temperature persistence. In the mid-latitudes of the North Atlantic, on the other hand, the covariance relationships between HFs are changing (negative covariances are decreasing) to produce a larger e relative to CTRL. The temperature persistence increases also in this area.

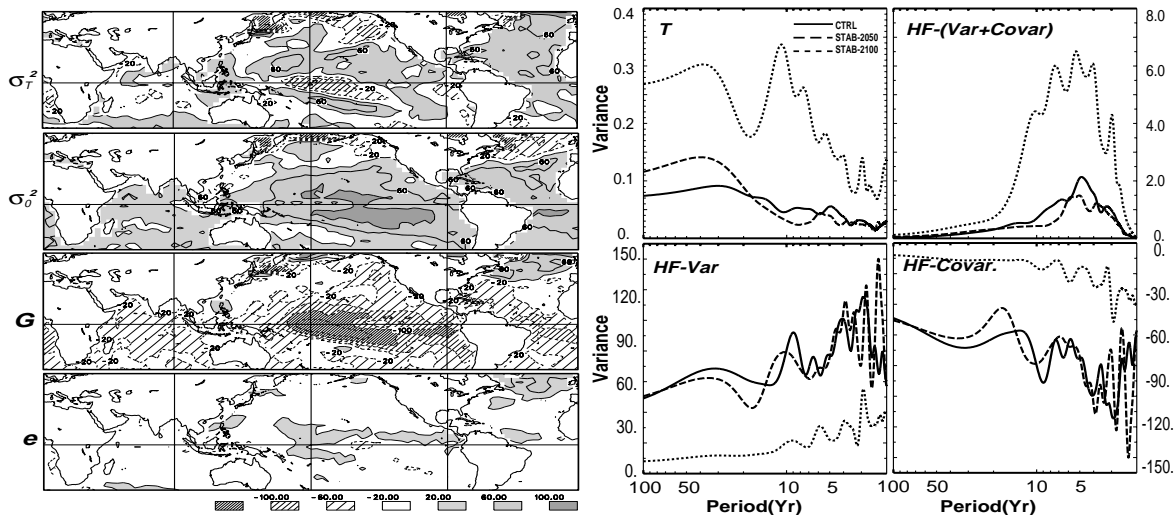


Figure 2 Percentage changes of SST variability with global warming (STAB-2100 relative to CTRL) and the associated variability balance.

Figure 3 Power spectra of the regional mean SST, HF and HF covariances from the model integrations, including CTRL, STAB-2050 and STAB-2100.

A power spectrum analysis over the mid-latitudes ($45\text{--}55^{\circ}\text{N}$) of the North Atlantic shows the relationship between temperature and HF variability in different timescales (Fig.3). In contrast to the increase of SST spectra, the spectra of the surface turbulent and ocean transport fluxes show significant decreases in the STAB-2100 warming scenario relative to the CTRL. This highlights again that it is the changes of HF covariances rather than HF variances alone that are responsible for the changes of temperature variability.

4. SUMMARY

SST variance is expressed as a combination of three factors: the sum of the variances of surface radiative and turbulent fluxes and the ocean heat transport, a transfer factor representing the SST persistence, and an efficiency factor associated with the covariance relationship among these terms. The geographical distribution of SST variance follows that of the sum of the variances of the heat fluxes but modified by a term reflecting the SST autocorrelation structure and an efficiency factor reflecting the covariance structure among the heat fluxes.

The changes of SST variability with GHG-induced warming show broad-scale features, which become more prominent with the increase of the external forcing and on longer timescales. Changes in different components of (1) gave the change in SST variability in different geographical regions and each plays an important role.

References

- Boer, G.J., 1993, Climate Dynamics, 8, 225-239.
- Boer, G.J. et al., 2000a, Climate Dynamics, 16, 405-425.
- Boer, G.J. et al., 2000b, Climate Dynamics, 16, 427-450.
- Flato, G.M. et al., 2000, Climate Dynamics, 16, 451-467.
- Kistler, R. et al., 2001, Bull AMS, 82, 247-268.
- Trenberth, K.E. et al., 2001, Climate Dynamics, 17, 259-276.
- von Storch H., and F. Zwiers, 1998, Cambridge University Press, 494pp.
- WCRP, 2000, WCRP-112, 303pp.
- Yu, B., and G.J. Boer, 2002, Climate Dynamics, in press.